ELSEVIER

Journal of Chromatography A, 924 (2001) 177–186

JOURNAL OF CHROMATOGRAPHY A

www.elsevier.com/locate/chroma

Shah convolution differentiation Fourier transform for rear analysis in microchip capillary electrophoresis

Yien C. Kwok, Andreas Manz*

AstraZeneca/SmithKline Beecham Centre for Analytical Sciences, Department of Chemistry, Imperial College of Science, Technology and Medicine, London SW7 2AY, UK

Abstract

This paper first reports the application of Shah convolution differentiation Fourier transform for rear analysis. Rear analysis eliminates the need to create a well-defined and reproducible sample plug, thus making the operation simpler. The number of solution reservoirs, for microchip capillary electrophoresis (CE), could be reduced from the usual four to three. Sample bias in CE could be avoided too. The separation channel was first filled with the fluorescent sample solution, and subsequently flushed out with the buffer. The rear of each analyte zone gives rise to its flight of sigmoid-shaped steps in the time-domain. The time-domain detector signal was first differentiated and then Fourier transform was performed. The Fourier transform results were represented in the form of a magnitude plot. It is proposed that this would be as equally applicable to other separation techniques (e.g., chromatography) and detection methods (e.g., absorption).

Keywords: Shah convolution differentiation Fourier transform; Chip technology; Rear analysis; Capillary electrophoresis; Instrumentation; Fourier transform; Rhodamine-110 chloride; Fluorescein

1. Introduction

Most detection techniques in separation science employ single-point detection – as each separated constituent analyte flows past the detection point, a signal is recorded. Spatial imaging, a form of multiple-point detection, in capillary zone electrophoresis allows the dynamic events along the capillary to be studied [1]; and when used in capillary isoelectric focusing, the mobilisation step required for single-point detection could be eliminated [2]. Spatial imaging could also improve S/N if coupled with signal-averaging [3,4]. This is especially important for detection in chip-based, small-volume capillary electrophoresis (CE) [5].

Alternatively, completely new methods, using mathematical and statistical techniques in combination with the mathematical and data-handling capabilities of computers, can be developed. This approach has been largely taken by analytical scientists over the last 2 decades to improve the S/N and/or resolution of many analytical techniques. Representing the usual time-domain electropherogram in the inverse-time domain has been shown to be advantageous for evaluating electrophoretic mobilities [6]. Economou et al. have employed Fourier transform (FT) and Hartley transforms to deconvolute overlapping chromatographic peaks [7]. Special mathematical techniques (e.g., sequences) could also be used to control the pattern of multiple sample injection. For

*Corresponding author. Fax: +44-207-5945-833.
E-mail address: a.manz@ic.ac.uk (A. Manz).

0021-9673/01/$ – see front matter
PII: S0021-9673(01)00989-X

example, in cross-correlation chromatography, the input flow of the column is rapidly switched between the sample and mobile phase in a pseudo-random pattern. The resulting random detector output is cross-correlated with the input pattern [8]. This has recently been demonstrated for microchip CE by Fister et al., with significant S/N enhancements within a relatively modest time [9]. Kaneta et al. injected the sample according to a pseudo-random Hadamard sequence [10]. Subsequent decoding using a corresponding inverse Hadamard matrix yielded an eightfold improvement in S/N owing to a high throughput of the signal. Szostek and Trojanowicz performed multiple, regular injection of the sample solution in a flow-injection system [11]. FT of the measured periodic signal resulted in a response related to concentration with improved S/N. These approaches still rely on the single-point detection.

A detection scheme comprising of a new method of column interrogation and a corresponding domain for analytical separation data presentation based on a convolution of the detection function similar to the Shah function, followed by FT was proposed by Crabtree et al. who named this technique as Shah convolution Fourier transform detection, or SCOFT [12]. During the separation, each analyte zone progressing along the column at its characteristic speed produces a series of evenly spaced Gaussian peaks, and the time-domain detector signal is thus the resultant sum of these several series of Gaussian peaks, n series for n analytes. A FT in the forward direction yields the frequency components contained in the time-domain detector signal. Further investigations aim to explore the full capabilities of this detection scheme. This work continues to explore SCOFT on a miniaturised total analysis system (μ-TAS) [13] device because it offers the obvious advantage in the ease with which the separation channels and detection array can be fabricated and aligned to each other. μ-TAS also offers real and expected benefits in terms of separation time, plate number, portability and automation, as well as reagent and instrumentation cost [14]. However, the final limit of miniaturisation systems will probably be set by the system detector since sample volumes of picolitre and optical path length of micrometre are commonly encountered [15]. SCOFT could be a method of circumventing these detection problems.

Frontal analysis has been applied in capillary electrophoresis and chromatography. It involves the injection of a sample volume relatively large compared to the capacity of the separation column. This led to the elution of analytes as distinct plateaus, followed by a resumption of detector baseline response. It is widely used in binding studies of various biomolecules of interest [16,17]. Gao et al. developed frontal analysis continuous capillary electrophoresis (FACCE) in which sample introduction and sample separation were integrated into one process [18]. Species separated appeared as discrete and progressive plateaus in the electropherograms. The separation profile of FACCE is particularly suitable for binding studies, in which the determination of the concentration of free or bound ligands without complete separation avoids perturbation of the binding equilibrium [18]. FACCE offers the edge over frontal analysis in terms of studying binding phenomenon with slow binding kinetics. These works still employed single-point detection.

In this work, unlike frontal analysis, the separation channel was first filled completely with the sample solution and subsequently flushed out with buffer by applying an electric field. The rear of each analyte zone was detected, hence termed ''rear analysis''. A novel detection scheme named Shah convolution differentiation Fourier transform (SCODFT) was employed. There are various associated advantages, for example, simpler design of the micromachined channel system for microchip CE, simpler control of sample introduction, and circumventing the problem of sample bias.

2. Experimental

2.1. Apparatus

Fig. 1 shows the box diagram of the instrumentation. The lenses, laser, chip, and electrodes were mounted with lens mounts or custom-made fixtures on carriers along a vertically mounted 2 m optical rail (lens mounts and posts on an X-95 rail and carrier system, Newport, Irvine, CA, USA); the photomultiplier tube (PMT) was mounted in a ring stand. The whole apparatus was enclosed in a light-tight galvanised steel box. A class 3B argon ion laser

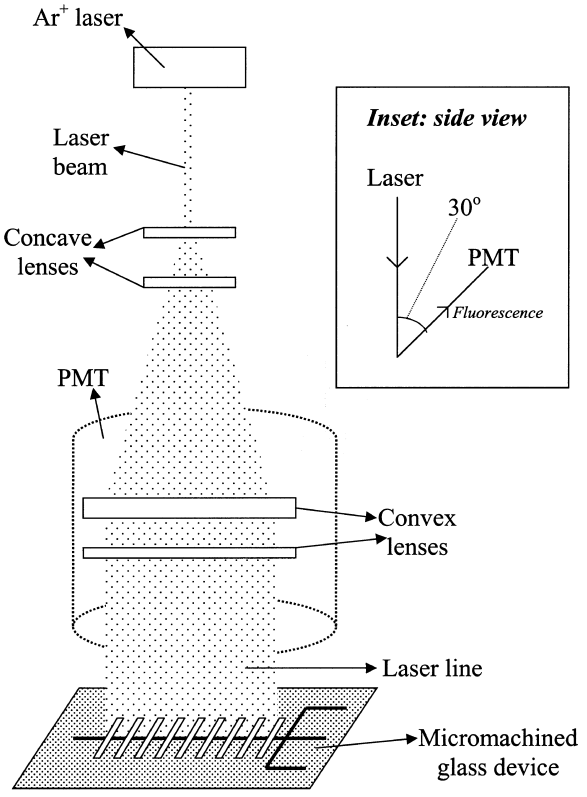

Fig. 1. Instrumental set-up (inset is the side-view of the set-up).

[line at 488 nm; Model 532-B-A01, OmNichrome (Melles Griot), Chino, CA, USA] was shone initially upon two concave cylindrical lenses (01LCN000, $f=-6.35$ mm; Melles Griot, Cambridge, UK) spaced 7 mm apart, to expand the beam, and then upon a convex cylindrical lens (01LCP013, $f=150$ mm; Melles Griot) 14 cm from the nearest concave lens above, producing a parallel beam expanded along one dimension to 4.5 cm (limited by the convex lens and holder) to cover the length of the separation channel. The beam then passed through a second convex cylindrical lens (01LCP009, $f=80$ mm, Melles Griot) with its cylindrical axis rotated 90° around the beam axis with respect to the previous lenses. This lens acted to focus the beam onto the width of the channel. The chip was positioned 9.3 cm beneath the lens to illuminate the full width of the channel. The chip was held in the apparatus with a locally built holder which fixes the chip in the optical path and the Pt electrodes in the reservoirs and provides high-voltage contacts for the electrodes.

Detection was performed with a 2 in. (1 in.=2.54 cm) head-on PMT (R550 PMT, E1198-11 socket, C3830 power supply, Hamamatsu Photonics, Middlesex, UK) with three high-pass interference filters (505EFLP, Omega Optical, Brattleboro, VT, USA), three high-pass Schott filters (OG515, Edmund Scientific, Barrington, NJ, USA), and one fluorescein emission band-pass filter (520DF15, Omega Optical) attached to the PMT, the last next to the PMT. The filter edges and PMT-filter interface were carefully foil-wrapped to eliminate unfiltered light from reaching the PMT. The PMT-filter assembly was mounted ca. 5.3 cm from the centre of the separation channel, at an angle of ca. 30° from the plane of the laser beam.

Current signal from the PMT biased at −1000 V was summed with an adjustable user-defined ''baseline-shift'' current, amplified with a current follower ($R_f=33$ MΩ), filtered with a single-stage active low-pass filter (194 Hz nominal cut-off frequency), and then acquired at 100 Hz (buffered) on an Apple Power Macintosh 9500/120 through a 16-bit data acquisition board (PCI-MIO-16XE-50, National Instruments, Berkshire, UK) with a program written in LabView 5.0 (National Instruments). Data manipulation and FT were performed on Igor Pro 3 (Wavemetrics, Lake Oswego, OR, USA) with Microsoft Excel 5.0 after acquisition.

Potentials at the four electrodes were controlled by a laboratory-made power supply, wherein discrete d.c.–d.c. converters (one per electrode) were regulated via multiplexing from another LabView program running on the same Apple Power Macintosh 9500/120. This allowed effective switching of all four electrodes in about 300 ms and electrical current sourcing or sinking at any electrode, as well as independent current and voltage monitoring.

2.2. Micromachined glass device

The micromachined glass device was manufactured at Micralyne (Edmonton, Canada) on Corning No. 0211 glass substrates (Corning, NY, USA). All channels were ca.15 μm deep, 50 μm wide at the top and 20 μm wide at the bottom. The 0.5-mm thick cover plate was thermally bonded to the substrate

and had 2-mm diameter holes drilled through for sample and reagent reservoirs. A 1000 Å chromium layer was plated and patterned on the top side of the cover plate to provide the detection slits. The 55 slits were each 300 μm wide and were spaced 700 μm centre to centre. Fig. 2 is a schematic diagram of the layout used in this work – a simple cross pattern of two intersecting channels and four reservoirs: (a) the sample injection channel with sample and sample waste reservoirs, and (b) the separation channel with buffer and buffer waste reservoirs, above which the detection slits lay. Reservoirs consisted of ca. 5 mm sections of micropipette tips epoxied to the glass surface around the 2 mm drilled holes, providing a reservoir volume of ca. 50 μl each. Channel lengths, measured from the intersection, were 3.62 cm to the sample reservoir, 3.92 cm to the buffer reservoir, 4.86 cm to the sample waste, and 6.60 cm to the buffer waste.

2.3. Reagents and solutions

Tris–borate–EDTA (TBE) buffer was prepared at 0.1× concentration (8.9 m*M* in both Tris and boric acid, 0.2 m*M* in ethylenediaminetetraacetic acid; prepared from a solid TBE mixture, Fluka) with deionised water (water purification system, Elga, Bucks., UK) and filtered through 0.2-μm filters (Millisart). Sodium fluorescein salt and Rhodamine-110 chloride were supplied by Fluka and Sigma–Aldrich, respectively. A 2-mg amount of each fluorescent dye was dissolved in 1 ml of ethanol with sonication. Appropriate volumes of the respective stock solutions were diluted with the 0.1× TBE buffer to make up a binary mixture of 100 μ*M* fluorescein and 25 μ*M* Rhodamine-110 chloride. Cleaning solution of 0.5 *M* sodium hydroxide was prepared from deionised water and sodium hydroxide (BDH).

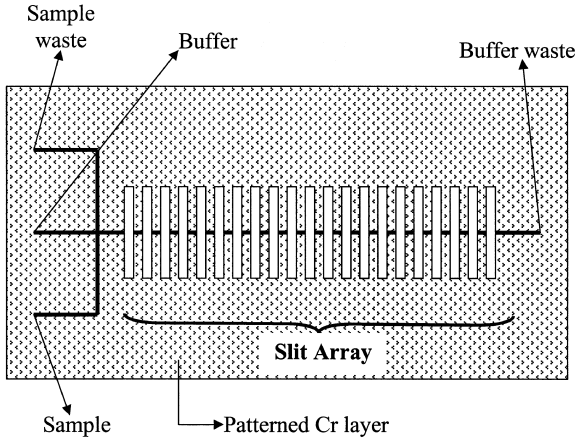

Fig. 2. A schematic diagram of the micromachined glass device showing the electrophoretic microchannels and the patterned Cr layer which provides the multiple detection windows.

2.4. Preparatory and experimental procedure

To prepare the chip, cleaning fluids were drawn into the chip by applying vacuum to one reservoir and supplying the other three with the appropriate fluid. Daily chip preparation consisted of drawing through 0.5 *M* NaOH followed by the running buffer, 0.1× TBE. The sample solution was then loaded into the sample reservoir, and the chip was ready to run. For overnight storage, the chip was filled with deionised water.

Flow optimisation under an inverted microscope (Leica DMIL equipped with a fluorescein filter cube and halogen lamp, Leica, Milton Keynes, UK) ensured that the separation channel was initially filled completely with the sample solution and subsequently flushed out with the buffer solution, and that no sample leakage occurred during the ''flush'' step. Fig. 3 is a schematic diagram of rear analysis. Table 1 shows the high-voltage protocol used in this work. The duration(s) of each step in the high-voltage protocol was optimised by ensuring a constant PMT signal was obtained when the separation channel was either filled or flushed of the sample solution. Once the high-voltage protocol had been executed correctly under the microscope at least twice, the chip's separation channel was filled with the fluorescent sample and immediately transferred to the detection apparatus. The chip was then aligned to the expanded laser beam with the translation stages, the box was closed and sealed, and following a flush of the separation channel of the fluorescent aligning solution, the whole high-voltage protocol was run while the time-domain signal was recorded.

Twenty slits were used for multiple-point detection, whereas single-point detection was performed

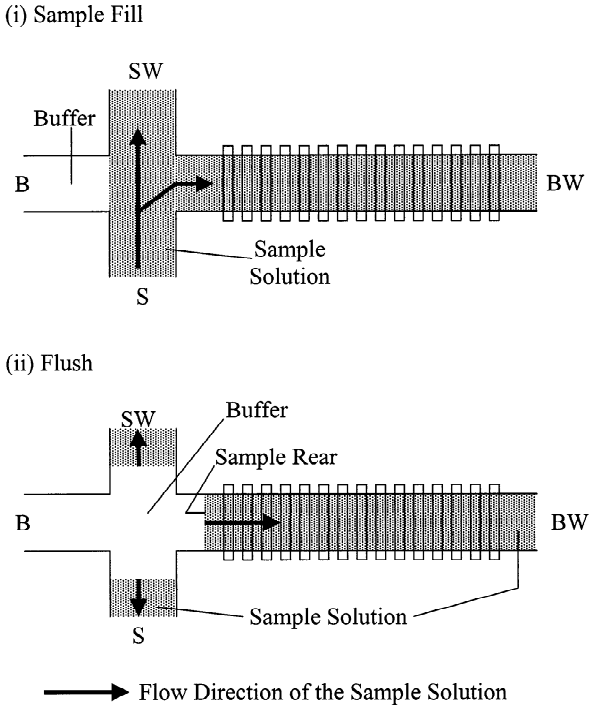

Fig. 3. A schematic diagram of rear analysis: (i) sample fill, (ii) flush. (S: Sample; SW: sample waste; B: buffer; BW: buffer waste).

by taping aluminium foil over all, except the 20th slit.

Data points were acquired and stored as text files in LabView and processed in Igor. Time, $t=0$ s for the time-domain detector signals was selected as the start of the ''flush'' step in Table 1. (The sigmoid-shaped signals, in the time-domain detector signals, were not distinct when the data was collected during the first step in Table 1 because the sample front became diffused after having travelled a considerable distance from the sample reservoir to the first slit. Conversely, the sample rear was less diffused and gave more distinct steps, hence termed ''rear analysis''). Data for an even number of points bracketing the relevant time span were then treated with a FT in the forward direction to yield the frequency-domain data. The FT algorithm yields $(N/2)+1$ complex points (pairs of real, $FT_{\nu,\,Re}$, and imaginary points, $FT_{\nu,\,Im}$) in the frequency domain for an input of N real points in the time domain.

3. Results and discussion

Fig. 4A shows the time-domain detector signals of the separation of a mixture of 100 μM fluorescein and 25 μM Rhodamine-110 chloride. A decreasing flight of sigmoid steps could be observed in the time-domain detector signals. The fluorescence, as detected by the PMT, would be a decreasing function as the fluorescent mixture moved out of the array of 20 detection slits. In addition, as a result of the presence of the equal-spaced slits, step-like structures would be expected as well. Diffusion leads to a slightly-diffused ''rear'' which is the cause of the sigmoid shape in each step, which would otherwise be decreasing linearly. In the first 11 s, the sigmoid steps could be roughly made out, but become clearer in the later half of the trace. The two sample rears separated owing to a difference in the electrophoretic mobilities of Rhodamine-110 chloride and fluorescein. Rhodamine-110 has a higher migration velocity than fluorescein. Therefore, the sample rear of Rhodamine-110 moved ahead of fluorescein's, and Rhodamine-110 chloride was the first of the two compounds to be flushed out of the detection array of 20 slits. In the process, each compound gave rise to its own individual series of sigmoid steps. The time-domain detector signals obtained was a summation of these two series, one from each compound. In the first 11 s, the sigmoid steps of both compounds

Table 1
Typical high-voltage program for a rear analysis experiment

Step	Reservoir potential (V)				Time (sec)
	Sample	Buffer	Sample waste	Buffer waste	
Sample fill	2000	1300	1300	0	60
Flush[a]	1000	2000	1000	0	60

[a] Data acquisition commenced at the start of this step, i.e., time = 0 s.

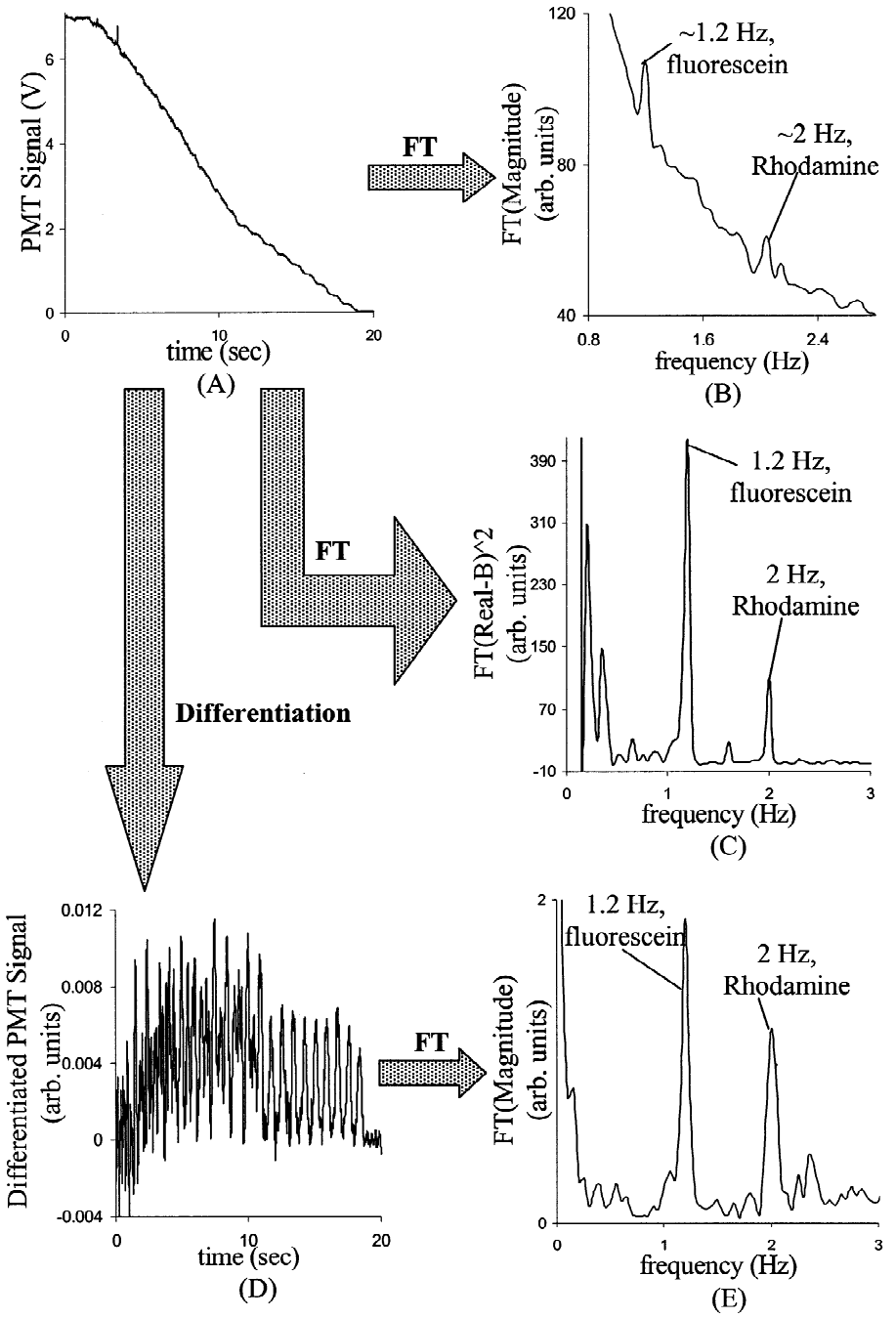

Fig. 4. For a separation of 100 μ*M* fluorescein and 25 μ*M* Rhodamine-110 chloride: (A) time-domain detector signals (detection with 20 slits). Conditions: 0.1× TBE buffer, pH 8.4; electric field strength 190 V/cm. (B) Magnitude plot of the FT of (A). (C) FT(Real$-B)^2$ plot of the FT of (A), and the value of *B* is 3.68. (D) Differentiated time-domain detector signal, by differentiating (A) with respect to time. (E) Magnitude plot of the FT of (D).

overlapped, thus the sigmoid steps are not distinct. After Rhodamine-110 chloride has exited the detection length, the sigmoid steps from fluorescein alone could be easily and clearly seen.

FT yields two sets of solutions, namely the real, FT(Real), and imaginary, FT(Imag). As was performed by Crabtree et al. [12], after FT, the magnitude plot, FT(Magnitude), was constructed, and the result is shown in Fig. 4B:

$$\mathrm{FT(Magnitude)} = \{[\mathrm{FT(Real)}]^2 + [\mathrm{FT(Imag)}]^2\}^{1/2} \quad (1)$$

Based on the fundamental frequencies obtained with each individual component, two peaks at 1.2 Hz (fluorescein) and 2 Hz (Rhodamine-110 chloride) could be roughly identified. However, the latter peak could also be mistaken as the noise in the magnitude plot. The frequencies of these two peaks could not be determined with certainty and accuracy because of the high level of noise and the strange peak shape. This would make future application and usage (for example, measurement of the frequency, and quantitation by peak height or area) difficult. It is unclear why such peak shape was obtained. Furthermore, the baseline was decreasing, thus making it more difficult to identify the existence of any peak and/or quantify. This is likely to be a result of the decreasing baseline in the time-domain. The overall decreasing baseline constitutes a non-periodic signal. Hence, the period tends towards infinity, and consequently the fundamental frequency tends to zero. The harmonics are more and more closely spaced and in the limit there is a continuum of harmonics, thereby giving rise to the decreasing baseline as observed in the frequency domain [19]. Therefore, this way of representation would not be useful in separation science. Alternative representations, with a constant baseline and desired peak shape in the frequency domain, were thus sought for.

The real solution, FT(Real), was then plotted out. The baseline was not decreasing, and two peaks were observed (roughly at 1.2 Hz and 2 Hz). The peak shape was similar to that observed in the magnitude plot. Being not useful, this plot is not shown. However, when the average value of the baseline in the real plot, *B*, was subtracted from the real solution and the result was then squared – see Eq. (2), satisfactory peak shape and baseline can be observed. This result is shown in Fig. 4C, $\mathrm{FT(Real}-B)^2$:

$$\mathrm{FT(Real} - B)^2 = \{[\mathrm{FT(Real)}] - B\}^2 \quad (2)$$

This gave exceptional S/N and two fundamental peaks of the usual shape at 1.2 and 2 Hz. The determination of the value of *B* was subjective, and *B* ranged from 3.16 to 3.68 for five similar separation runs. Thus, the peak height would be highly dependent on the subjective determination of the values of *B*. In the separation experiment using the $\mathrm{FT(Real}-B)^2$ plot, the height of the fluorescein fundamental peak ranged from 325 to 625 arbitrary units (standard deviation = 125; RSD = 27.5% for n = 5), while the height of the Rhodamine-110 chloride fundamental peak ranged from 60 to 120 arbitrary units (standard deviation = 28.3; RSD = 35% for n = 5). Subsequent comparison with the single-point detected electropherogram shows that the ratios of peak heights do not match. This will be presented and discussed later. In addition, FT results are commonly represented as phase or magnitude plots. No physical meaning could be associated with this plot, $\mathrm{FT(Real}-B)^2$, though satisfactory results seemed to be obtained.

The imaginary solution, FT(Imag), of the FT was next considered. The result was similar to the magnitude plot, and thus is not shown. Squaring FT(Imag) would not give a significantly different result. The baseline and peak shape are not satisfactory, thus making these two ways of representation not useful in separation science.

Numerical differentiation with respect to time of the time-domain detector signals (Fig. 4A) was performed. This resulted in a series of inverted peaks which were then reversed; it should be noted that the subsequent FT results were found to be the same. The end result (after the reversal, but prior to FT) is shown in Fig. 4D. A series of positive peaks was obtained. Peaks were hardly discernible in the first 11 s of the time-domain detector signals. As discussed earlier, this part represented the period when both compounds were in the detection array of 20 slits, and hence would be a summation of the two series of signals, one due to each compound. Once Rhodamine-110 chloride, the faster moving component, has exited, the peaks due to fluorescein could be readily seen in the later half of Fig. 4D. Sub-

sequent FT was performed and the result was presented as the magnitude plot (Fig. 4E). The baseline was not decreasing because differentiation removes the non-periodic, decreasing baseline in the original time-domain detector signals. Two fundamental peaks, 1.2 Hz for fluorescein and 2 Hz for Rhodamine-110 chloride, could be clearly seen. In addition, there is a small first harmonics for fluorescein at 2.4 Hz; there is no observable first harmonics for Rhodamine-110 chloride at 4 Hz (not shown). The shapes of both peaks were satisfactory. The variation in peak heights were very much smaller compared to that for FT(Real$-B)^2$ plot (without prior differentiation). The height of the fluorescein fundamental peak ranged from 1.75 to 1.9 arbitrary units (standard deviation = 0.07; RSD = 3.5% for n = 5), while the height of the Rhodamine-110 chloride fundamental peak ranged from 1.1 to 1.4 arbitrary units (standard deviation = 0.13; RSD = 9.8% for n = 5). The ratio of peak heights was clearly different from the ratio in FT(Real$-B)^2$ plot (without prior differentiation) in Fig. 4C. However, direct comparison cannot be made because the two plots are totally different. Therefore, it is proposed that prior differentiation, followed by FT and using the magnitude plot, is the best data processing procedure for rear analysis. The name, Shah convolution differentiation Fourier transform, is thus proposed.

Single-point detection was performed for a rear analysis separation of the same mixture of 100 μ*M* fluorescein and 25 μ*M* Rhodamine-110 chloride. The electropherogram is shown in Fig. 5. The first drop in the measured fluorescence (at around 10.5 s) was caused by the exit of the faster-moving component, Rhodamine-110 chloride; this was followed by fluorescein which resulted in the second drop in the measured fluorescence at around 18 s. Three similar runs of the separation were done. The use of the height of the step/plateau for quantitation had been demonstrated by Gao et al. [18]. From these single-point detected electropherograms, the ratio of heights of the steps of Rhodamine-110 chloride to fluorescein was calculated. It was found to be an average of 0.61 with a standard deviation of 0.05 for three similar runs. The ratio of the fundamental peak heights in the magnitude plot, Fig. 4E, was calculated. By this method, the average ratio was found to be 0.66 with a standard deviation of 0.1 for five similar runs. Student's *t*-test was performed and revealed that there was no statistical difference in the results by these two methods at 95% confidence level. A similar calculation was performed for Fig. 4C. The average ratio was 0.18 with a standard deviation of 0.08 for five similar runs. Student's *t*-test showed that there exists a significant statistical difference. This indicates that the information contained in Fig. 4E is more likely to reflect the true concentrations and characteristics of all the analytes in the mixture than the other plots. Therefore, this further confirms the feasibility and applicability of SCODFT as the detection and data-processing scheme for rear analysis.

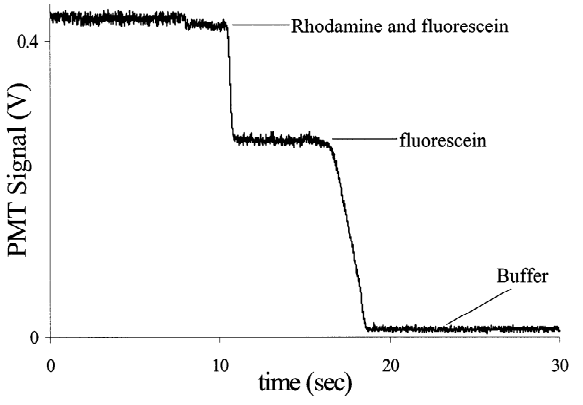

Fig. 5. Electropherogram (with single-point detection) for a rear analysis separation of 100 μ*M* fluorescein and 25 μ*M* Rhodamine-110 chloride. Conditions: 0.1× TBE buffer, pH 8.4; electric field strength 190 V/cm; detection at the 20th slit.

Visual comparison between Figs. 4E and 5 showed an apparent deterioration of S/N by performing multiple-point detection. S/N enhancement is expected, by virtue of detection at multiple points [19]. The reason for this unexpected trend is unclear, though non-optimised optics was suspected to be a contributing factor.

Resolving two closely-spaced steps visually could prove to be difficult as the transition from one step to another could be easily missed. Comparatively, where the shape of the analytical signals is similar to Fig. 4E, the ''valley'' between two adjacent peaks could be more easily identified. Numerical differentiation of Fig. 5 with respect to time was performed, and the result is shown in Fig. 6. The signal of Rhodamine-110 chloride became greater than

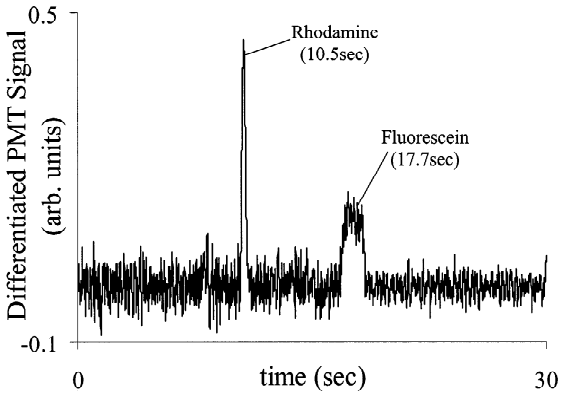

Fig. 6. Differentiated time-domain detector signal (single-point detection), by differentiating Fig. 5 with respect to time.

fluorescein's. In addition, a drastic reduction in S/N for the signal of fluorescein was observed. This is because, if differentiation was only performed, the peak height is proportional to the gradient of the decreasing part of each step. In turn, the gradient is related to the speed at which each sample rear moved across the single detection window. Therefore, the peak height is related to the migration velocity of each analyte, and could not be employed for quantitation or calibration.

4. Conclusion

The results of the application of SCODFT to rear analysis are first reported in this paper. The applicability and feasibility of SCODFT were successfully demonstrated for a separation of two fluorescent compounds.

It has long been known that reproducible injection of a very small volume of sample solution is difficult. Rear analysis eliminates the need to inject a small and reproducible volume of sample plug for interrogation by the detection function (i.e., Shah). The usual number of solution reservoirs for microchip CE could be reduced from four to three, and hence a simpler layout of the microchannel system [20]. That also means that the number of parameters to control for proper and reproducible sample solution flow is reduced, making the operation simpler. Sample bias, common with electrokinetic injection in conventional capillary electrophoresis, could be avoided by acquiring the time-domain detector signal until constant baselines are obtained on both sides of the flight of sigmoid steps – this ensures that the slowest-moving component would have been completely interrogated by the detection function (i.e., Shah).

The expected S/N enhancement was not apparent, and future work would identify the cause. If detection were performed with only one slit, the analytical signals would be in the form of steps, which could hinder the visual resolution of two closely-spaced steps. Though the shape of the analytical signal (by single-point detection) could be altered by differentiation, the peak height would not be useful for quantitation. SCODFT transformed the shape of the analytical signal, thereby making visual resolution of the fundamental peaks easier; and the height of the fundamental peak relates to the concentration. Future work could compare the resolution by choosing two similar and closely-separated compounds, and further demonstrate the separation capability with more than two compounds. Establishing the calibration plot would also be of interest. Though the sample rear was detected and analysed in this work, SCODFT is equally applicable for frontal analysis (e.g., as in FACCE).

Acknowledgements

The authors wish to thank Micralyne (Edmonton, Canada) for fabricating the micromachined glass device used in this work, and AstraZeneca and SmithKline Beecham. Y.C.K. would like to express his sincerest gratitude to Dr. H.J. Crabtree for his help and guidance in the project, and the micromachined glass device. Y.C.K. thanks Drs. J. Eijkel, D. Reyes, G. Sanders, R. Tantra and C.-X. Zhang for all the insightful discussions. Y.C.K. acknowledges the funding from the Overseas Research Student Awards Scheme, and the financial support from his parents.

References

[1] T. Johansson, M. Petersson, J. Johansson, S. Nilsson, Anal. Chem. 71 (1999) 4190.

[2] Q.L. Mao, J. Pawliszyn, J. Biochem. Biophys. Methods 1–2 (1999) 93.
[3] C.T. Culbertson, J.W. Jorgenson, Anal. Chem. 70 (1998) 2629.
[4] C.T. Culbertson, J.W. Jorgenson, J. Microcol. Sep. 11 (1999) 652.
[5] D.J. Harrison, K. Fluri, K. Seiler, Z. Fan, C.S. Effenhauser, A. Manz, Science 261 (1993) 895.
[6] M. Mammen, I.J. Colton, J.D. Carbeck, R. Bradley, G. Whitesides, Anal. Chem. 69 (1997) 2165.
[7] A. Economou, P.R. Fielden, A.J. Packham, Analyst 121 (1996) 97.
[8] J.N. van der Moolen, H. Poppe, H.C. Smit, Anal. Chem. 69 (1997) 4220.
[9] J.C. Fister, S.C. Jacobson, J.M. Ramsey, Anal. Chem. 71 (1999) 4460.
[10] T. Kaneta, Y. Yamaguchi, T. Imasaka, Anal. Chem. 71 (1999) 5444.
[11] B. Szostek, M. Trojanowicz, Chemomet. Intell. Lab. Syst. 22 (1994) 221.
[12] H.J. Crabtree, M.U. Kopp, A. Manz, Anal. Chem. 71 (1999) 2130.
[13] A. Manz, N. Graber, H.M. Widmer, Sens. Actuators B 1 (1990) 244.
[14] M.U. Kopp, H.J. Crabtree, A. Manz, Curr. Opin. Chem. Biol. 1 (1997) 410.
[15] W.E. van der Linden, Trends Anal. Chem. 6 (1987) 37.
[16] N.A.L. Mohamed, Y. Kuroda, A. Shibukawa, T. Nakagawa, S. El Gizawy, H.F. Askal, M.E. El Kommos, J. Chromatogr. A 875 (2000) 447.
[17] A. Shibukawa, Y. Kuroda, T. Nakagawa, J. Pharm. Biomed. Anal. 18 (1999) 1047.
[18] J.Y. Gao, P.L. Dubin, B.B. Muhoberac, Anal. Chem. 69 (1997) 2945.
[19] J.F. James, A Student's Guide To Fourier Transforms: With Applications in Physics and Engineering, Cambridge University Press, Cambridge, 1995.
[20] D.J. Harrison, A. Manz, Z. Fan, H. Ludi, H.M. Widmer, Anal. Chem. 64 (1992) 1926.